

Revision of model parameters for β -type charge transfer salts: an ab initio study.Hem C. Kandpal,¹ Ingo Opahle,¹ Yu-Zhong Zhang,¹ Harald O. Jeschke,¹ and Roser Valent¹¹Institut für Theoretische Physik, Goethe-Universität Frankfurt,
Max-von-Laue-Strasse 1, 60438 Frankfurt am Main, Germany

(Dated: February 21, 2024)

Intense experimental and theoretical studies have demonstrated that the anisotropic triangular lattice as realized in the β -(BEDT-TTF)₂X family of organic charge transfer (CT) salts yields a complex phase diagram with magnetic, superconducting, Mott insulating and even spin liquid phases. With extensive density functional theory (DFT) calculations we refresh the link between manybody theory and experiment by determining hopping parameters of the underlying Hubbard model. This leads us to revise the widely used semiempirical parameters in the direction of less frustrated, more anisotropic triangular lattices. The implications of these results on the system's description are discussed.

PACS numbers: 74.70.Kn, 71.10.Fd, 71.15.Mb, 71.20.Rv

A strong research trend of the new millennium has been the desire to understand complex manybody phenomena like superconductivity and magnetism by realistic modelling, i.e. to employ precise first principles calculations to feed the intricate details of real materials into the parameter sets of model Hamiltonians that are then solved with increasingly powerful manybody techniques. The β -(BEDT-TTF)₂X [1] organic charge transfer salts are a perfect example for a class of materials with such fascinating properties that they drive progress in experimental and manybody methods alike. Experimentally, the phase diagram shows Mott insulating, superconducting, magnetic and spin liquid phases [2, 3, 4, 5]. Theoretically, the underlying anisotropic triangular lattice is a great challenge due to effects of frustration and the intense efforts to get a grip on the problem include studies with path integral renormalization group (PIRG) [6], exact diagonalization [7], variational Monte Carlo [8], cluster dynamical mean field theory [9, 10] and dual Fermions [11] to cite a few. In this rapidly expanding field of research, electronic structure calculations play the decisive role of mediating between the complex underlying structure and phenomenology of organic charge transfer salts and the models used for understanding the physics [12], and in this work, we will provide the perspective of precise, state of the art electronic structure calculations.

Previously, β -type CT salts have been investigated by semiempirical and first principles electronic structure calculations. The most commonly used t , t' , U parameter sets derive from extended Hückel molecular orbitals calculations [13, 14] performed on different constellations of BEDT-TTF dimers.

The main result reported here is that our first principles study shows all four considered β -type CT salts to be less frustrated than previously assumed based on semiempirical theory. Most importantly, the often cited value of $t^0/t = 1.06$ [13] for the spin liquid material β -(ET)₂Cu₂(CN)₃ should be replaced by the significantly

smaller value $t^0/t = 0.83 - 0.08$. This has fundamental implications on the system's model description as we shall see below.

In this Letter, we employ the Car-Parrinello [15] projector-augmented wave [16] molecular dynamics (CPMD) method for relaxing the only partially known structures and perform structure optimizations at constant pressure [17] in order to prepare high pressure structures. We calculated the electronic structure using two full potential all-electron codes, the linearized augmented plane wave (LAPW) method implemented in WIEN2K [18] and the full potential local-orbital (FPLO) method [19].

We base our study on the following structures: For β -(BEDT-TTF)₂Cu₂(CN)₃, the crystal structure [20] was published without hydrogen atom positions; we add them and perform a CPMD relaxation within the generalized gradient approximation (GGA) in which we keep lattice parameters and heavy atom (S, Cu) positions fixed [21]. With this procedure we make sure that the important atomic positions in the crystal structure remain as given by the diffraction measurements. We remove the inversion center in the middle of a cyano group by lowering the symmetry from $P2_1/c$ to Pc . No high pressure structures of β -(BEDT-TTF)₂Cu₂(CN)₃ are published, and we therefore perform a full relaxation of the structure and lattice parameters at a pressure $P = 0.75$ GPa [22]; we recover the Pc symmetry by further optimizing the high pressure structure with symmetry constraints. For β -(BEDT-TTF)₂Cu(SCN)₂, structures at ambient pressure and at $P = 0.75$ GPa are known [23]. Ambient pressure structures are available for β -(BEDT-TTF)₂Cu[N(CN)₂Br] [24, 25] and β -(BEDT-TTF)₂Cu[N(CN)₂Cl] [26]. We will refer to the four materials as β -CN, β -SCN, β -Br and β -Cl for brevity. At ambient pressure and low temperatures β -SCN and β -Br superconduct while β -Cl orders antiferromagnetically.

As an example for the structure of all β -type CT salts considered here, we show in Fig. 1 the structure of β -CN.

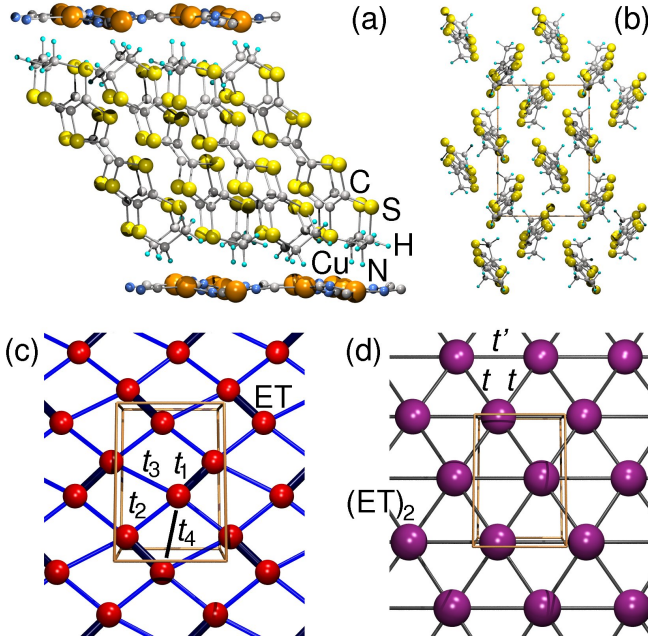


FIG. 1: (Color online) Structure of κ -(BEDT-TTF) $_2$ Cu $_2$ (CN) $_3$ as typical example of the κ -type CT salts. (a) Side view with ET layers separated by insulating Cu $_2$ (CN) $_3$ anion layers. (b) ET lattice, viewed in the bc plane. The unit cell containing four ET molecules is shown. (c) ET lattice shown in the same projection as (b) where the ET molecules have been replaced by single spheres. ET dimers are emphasized by heavier bonds. (d) Lattice of ET dimers, replaced by single spheres.

The strongly anisotropic nature of the materials is apparent from the alternation of charge donating ET layers and acceptor anion layers (Fig. 1 (a)), Cu $_2$ (CN) $_3$ in this case. Experimental observations [13] as well as our calculations show that Cu occurs in Cu $^{+1}$ oxidation state here and has a filled 3d shell, making the anion layers insulating. The κ -type arrangement of ET molecules (Fig. 1 (b)) exhibits a strong dimerization of the molecules, four of which are contained in a unit cell. They form the lattice shown in simplified form in (Fig. 1 (c)). In the charge transfer process, each molecule donates a charge of 0.5e and is left with half a hole. Considering pairs of dimers as the fundamental unit leads to the triangular lattice of Fig. 1 (d) with one hole per dimer.

In Fig. 2 we show three examples of low energy bandstructures for κ -CN at ambient and elevated pressure (Fig. 2 (a)) and for κ -Cl (Fig. 2 (b)). The overall features of the bandstructures are very similar to the known semiempirical band structures, with two antibonding bands of the ET molecules crossing the Fermi level, and the corresponding bonding bands nearly mirror symmetric below. Due to the double number of eight ET molecules per unit cell in the case of κ -Cl, Fig. 2 (b) actually has four bands crossing the Fermi level, which are pairwise degenerate due to the high symmetry (Pnma)

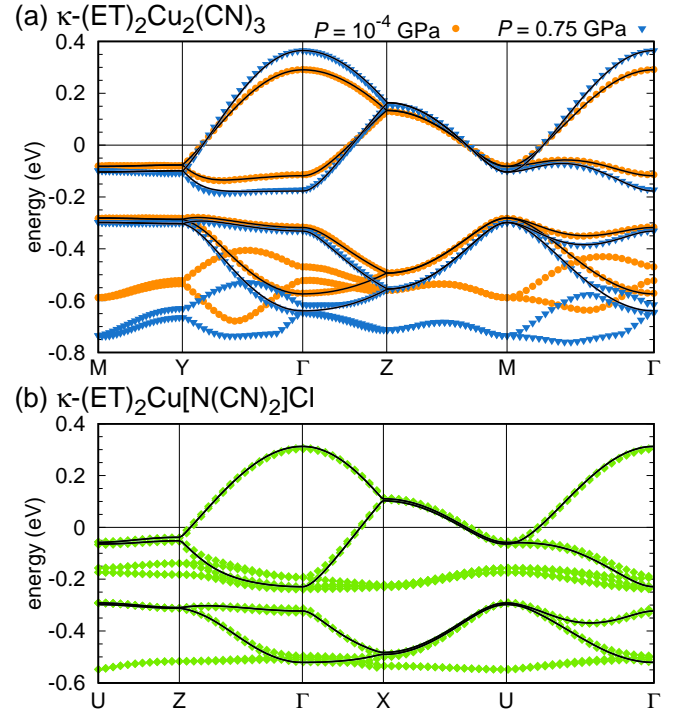


FIG. 2: (Color online) DFT bandstructures of (a) κ -(BEDT-TTF) $_2$ Cu $_2$ (CN) $_3$ at ambient pressure and at $P = 0.75$ GPa, and of (b) κ -(BEDT-TTF) $_2$ Cu[N(CN) $_2$]Cl shown with symbols. Lines represent the tight binding fits to the bands close to E_F deriving from ET molecules.

of the crystal structure. In contrast to previous calculations, there are four bands with mainly Cu 3d character close to the ET bands; slightly below the bonding ET bands in the case of κ -CN and slightly below the antibonding ET bands in the case of κ -Cl. The bandstructures of Fig. 2 (a) were performed with LAPW using the GGA functional [27]. We checked the reliability and reproducibility of these results by repeating the calculation with FPLO [29], and we found that the band structures and all derived quantities match very well. As κ -Cl has roughly twice as many atoms in the unit cell compared to κ -CN, we used the faster FPLO method, with GGA, for Fig. 2 (b). The low energy bands show almost no dispersion in the direction perpendicular to the anion layers which is the a direction (M-Y in the Brillouin zone) for κ -CN and the b direction (U-Z in the Brillouin zone) for κ -Cl, confirming the quasi-two-dimensional character of the κ -type CT salts.

We corroborated that the calculated bandstructures agree with experimental evidence by calculating the Fermi surface (FS) for κ -CN at ambient pressure and at $P = 0.75$ GPa. The FS consists of two different sheets arising from the two bands crossing the Fermi energy, a corrugated cylinder around Z and a quasi one dimensional sheet parallel to M-Y. Both sheets touch along the line M-Z and give rise to a combined elliptical orbit

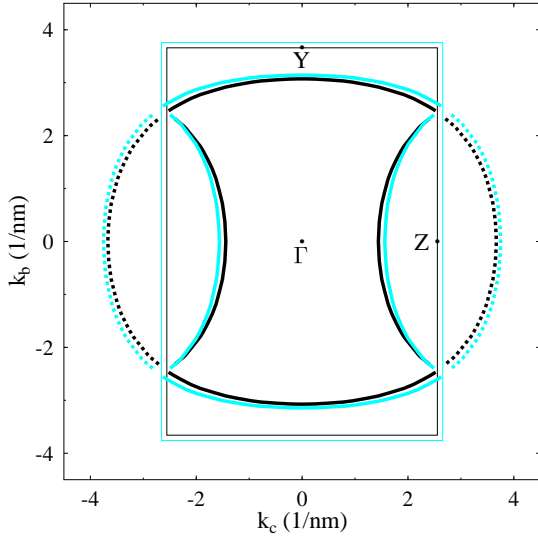


FIG. 3: (Color online) Fermi surface cuts for nonmagnetic $-(\text{BEDT-TTF})_2\text{Cu}_2(\text{CN})_3$ at ambient pressure (black) and at $P = 0.75$ GPa (light). Thin lines show the respective first Brillouin zone. The combined elliptical orbit as detected by AMRO measurements (see text) is indicated by broken lines.

(Fig. 3) which encloses 99–100% of the area of the first Brillouin zone. This is in good agreement with previous calculations [13] and with angle-dependent magnetoresistance oscillations (AMRO) measurements [30]. Our calculated FS shows the same behavior with pressure as observed in experiment. The area enclosed by the combined elliptical orbit increases by 6% from 37.4 nm^2 at ambient pressure to 39.7 nm^2 at $P = 7.5$ kbar (see Fig. 3), which is consistent with the increase of 6% between 2.1 and 7 kbar obtained from AMRO measurements in Ref. [30].

In the next step, we use the DFT band structures to extract the parameters of the Hubbard Hamiltonian

$$H = \sum_{\langle ij \rangle} t(c_i^\dagger c_j + \text{H.c.}) + \sum_{[ij]} t^0(c_i^\dagger c_j + \text{H.c.}) + U \sum_i n_{i\uparrow} \frac{1}{2} n_{i\downarrow} \frac{1}{2} :$$

where $\langle ij \rangle$ and $[ij]$ indicate sum over nearest and next nearest neighbors, respectively. We do this by fitting the bands to a tight binding model. Note that also nonlocal correlations V , V^0 are thought to play a role in organic CT salts but their determination is beyond the scope of our present investigation. We consider each molecule position as shown in Fig. 1 (c) as a site; then the four (eight) sites per unit cell contribute the four (eight) ET bands at the Fermi level in the case of $-\text{CN}$ and $-\text{SCN}$ ($-\text{Br}$ and $-\text{Cl}$). This yields the hopping integrals t_1 to t_4 where the index indicates increasing distance; t_1 is the intradimer hopping integral. The black lines in Fig. 2 show as an example the tight-binding t obtained from

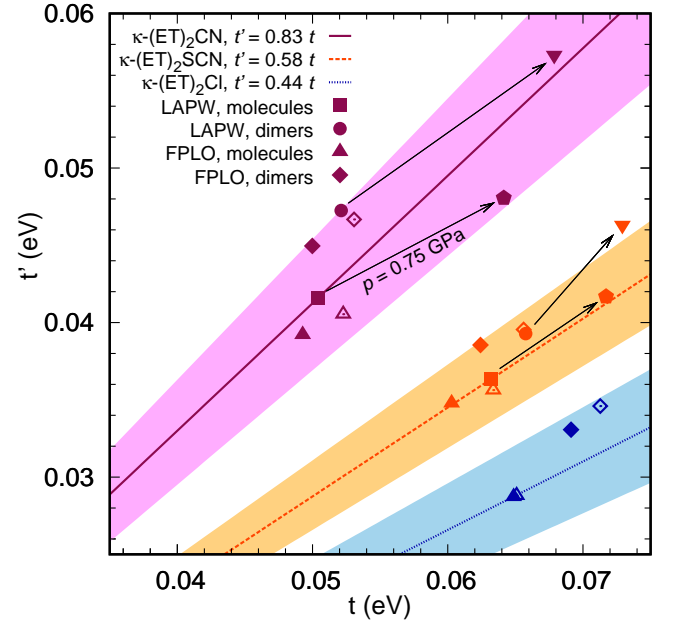


FIG. 4: (Color online) Overview of hopping parameters obtained from GGA (filled symbols) and LDA (open symbols) calculations for $-(\text{BEDT-TTF})_2\text{Cu}_2(\text{CN})_3$, $-(\text{BEDT-TTF})_2\text{Cu}(\text{SCN})_2$ and $-(\text{BEDT-TTF})_2\text{CuN}(\text{CN})_2\text{Cl}$. The spread of t and t^0 parameters depending on basis set, functional and number of fitted bands yields t^0/t ratios with a margin of error indicated by lines and shaded regions. Arrows indicate the change of t^0/t ratio due to application of a pressure of $P = 0.75$ GPa.

the molecular model. We follow Ref. 13 in the use of the geometrical formulas $t = (t_2 + t_4)/2$ and $t^0 = t_3/2$ for obtaining t and t^0 of Eq. 1. In order to corroborate these results, we use the alternative method of considering the ET dimers as sites of the tight binding model as shown in Fig. 1 (d). Then the two dimers per unit cell for $-\text{CN}$ and $-\text{SCN}$ are responsible for the two antibonding ET bands at the Fermi level (or four dimers/four antibonding bands in the case of $-\text{Br}$ and $-\text{Cl}$).

The result of these extensive bandstructure calculations and tight binding fits is summarized in Fig. 4. The choice of basis set (LAPW or FPLO), functional (GGA or LDA) and number of sites included in the fit (molecules or dimers) results in a certain spread of resulting t , t^0 pairs which we interpret as a margin of error. The slopes of the lines connecting the origin with the tight binding results for the GGA bands [31] show the results for the t^0/t ratios at ambient pressure: $t^0/t = 0.83 \pm 0.08$ for $-\text{CN}$, $t^0/t = 0.58 \pm 0.05$ for $-\text{SCN}$, $t^0/t = 0.44 \pm 0.05$ for $-\text{Cl}$, and $t^0/t = 0.42 \pm 0.08$ for $-\text{Br}$.

With the tight binding results, we can estimate the Hubbard U as $U = 2t_1$ following Ref. [32]. We obtain U/t ratios of $U/t = 7.3$ for $-\text{CN}$, $U/t = 6.0$ for $-\text{SCN}$, $U/t = 5.5$ for $-\text{Cl}$ and $U/t = 5.1$ for $-\text{Br}$. These values provide a readjustment of the position of the four

-type CT salts in the ($U=t$; $t^0=t$) phase diagram, compared to the semiempirical calculations: For -CN, we replace (8.2; 1.06) by (7.3; 0.83), for -SCN (6.8; 0.84) by (6.0; 0.58), for -Cl (7.5; 0.75) by (5.5; 0.44) and for -Br (7.2; 0.68) by (5.1; 0.42). At $P = 0.75$ GPa, we have (6.0; 0.75) for -CN and (5.7; 0.58) for -SCN.

In Fig. 4 we also show the analysis of pressure effects on the t , t^0 parameters. We represented with arrows the parameter changes from the ambient pressure results to the $P = 0.75$ GPa results in -SCN and -CN. For -CN, pressure leads to a decrease in the $t^0=t$ ratio, while we observe almost constant $t^0=t$ for -SCN. On the other hand we can establish that the parameter differences among the three studied cases at ambient pressure can be attributed to internal chemical pressure due to the different anion sizes. By comparing the ratios $t^0=t$ for -CN, -SCN and -Cl at ambient pressure with the physical pressure $t^0=t$ behavior for -CN and -SCN we observe that chemical pressure and physical pressure have the same effect on the $t^0=t$ ratio: for -CN, pressure significantly decreases the $t^0=t$ ratio. This effect is weaker for -SCN.

We now consider the new positioning of the four -type CT salts in some of the calculated ($U=t$; $t^0=t$) phase diagrams. In the PIRG phase diagram of Ref. 6, -Cl are shifted from the nonmagnetic insulating (NMI) phase to the antiferromagnetic insulating (AFI) phase which is an improvement as the superconducting phase is not considered in this work. Meanwhile, -CN and -SCN are only repositioned within the NMI phase. In the CDMFT phase diagram of Ref. 9, -Br is moved from the AF phase to the d-wave superconducting (SC) phase; -Cl is moved from the spin liquid (SL) phase to the border between AF and d-wave superconducting (SC) phase. -CN is moved from the d-wave SC phase to the border between SL and SC phases, and -SCN is moved within the SC phase. The effect of pressure means that -CN is moved diagonally across the SC phase by the application of $P = 0.75$ GPa. In particular, the positions of -Br, -Cl and -CN in the phase diagram are clearly improved. Our results exclude the possibility of viewing -CN as a quasi-one-dimensional system [33].

In conclusion, we have presented the results of density functional theory calculations for four -type charge transfer salts. We obtain important shifts of the familiar $t^0=t$ ratios from semiempirical electronic structure calculations [13] towards significantly smaller values, i.e. towards lower frustration. Due to the smaller overall bandwidth of the ET bands at the Fermi level, our estimate for the $U=t$ values is also below the prevalent values. Our results call for a reexamination of the description of the -type charge transfer salts, and in particular for -CN, namely which is the nature of the spin liquid at ambient pressure as well as the phase transition from Mott insulator to superconducting state under pressure.

Note added: While finalizing this manuscript, Nakamura et al. [34] have posted a manuscript, where similar values of $t^0=t$ for -CN and -SCN as in our full-potential calculations are obtained from a pseudopotential method.

We acknowledge useful discussions with L. Tocchio and C. Gros. We thank the Deutsche Forschungsgemeinschaft for financial support through the TRR/SFB 49 and Emmy Noether programs and we acknowledge support by the Frankfurt Center for Scientific Computing.

Electronic address: jeschke@itp.uni-frankfurt.de

- [1] BEDT-TTF, or shorter ET, stands for bis(ethylene-dithio)tetrathiafulvalene.
- [2] H. Elsinger et al., Phys. Rev. Lett. 84, 6098 (2000).
- [3] Y. Shimizu et al., Phys. Rev. Lett. 91, 107001 (2003).
- [4] Y. Kurosaki et al., Phys. Rev. Lett. 95, 177001 (2005).
- [5] F. Kagawa et al., Nature 436, 534 (2005).
- [6] H. Morita et al., J. Phys. Soc. Jpn. 71, 2109 (2002).
- [7] R. T. Clay et al., Phys. Rev. Lett. 101, 166403 (2008).
- [8] T. Watanabe et al., J. Phys. Soc. Jpn. 75, 074707 (2006), and Phys. Rev. B 77, 214505 (2008).
- [9] B. Kyung, A.-M. S. Tremblay, Phys. Rev. Lett. 97, 046402 (2006).
- [10] T. Ohashi et al., Phys. Rev. Lett. 100, 076402 (2008).
- [11] H. Lee et al., Phys. Rev. B 78, 205117 (2008).
- [12] B. J. Powell, R. H. McKenzie, J. Phys.: Condens. Matter 18, R827 (2006).
- [13] T. Komatsu et al., J. Phys. Soc. Jpn. 65, 1340 (1996).
- [14] A. Fortunelli, A. Painelli, J. Chem. Phys. 106, 8051 (1997), and Phys. Rev. B 55, 16088 (1997).
- [15] R. Car, M. Parrinello, Phys. Rev. Lett. 55, 2471 (1985).
- [16] P. E. Blochl, Phys. Rev. B 50, 17953 (1994).
- [17] M. Parrinello, A. Rahman, Phys. Rev. Lett. 45, 1196 (1980).
- [18] P. Blaha et al. WIEN2K, An Augmented Plane Wave + Local Orbitals Program for Calculating Crystal Properties (Karlheinz Schwarz/Techn. Universität Wien, Wien, Austria, 2001).
- [19] K. Koepf, H. Eschrig, Phys. Rev. B 59, 1743 (1999); <http://www.FPLO.de>
- [20] U. Geiser et al., Inorg. Chem. 30, 2586 (1991).
- [21] For CP-PAW, we employ a (4 4 4) k mesh and plane wave cutoffs of 60 Ryd and 240 Ryd for the wavefunction and charge density, respectively.
- [22] In the constant pressure [17] CPM D method, the pressure P directly enters the Lagrangian for the lattice dynamics as a term P with unit cell volume.
- [23] M. Rahalet al., Acta Cryst. B 53, 159 (1997).
- [24] U. Geiser et al., Acta Cryst. C 47, 190 (1991).
- [25] A. M. Kiani et al., Inorg. Chem. 29, 2555 (1990).
- [26] J. M. Williams et al., Inorg. Chem. 30, 3272 (1990).
- [27] For LAPW, we employ a (5 10 7) k mesh in the irreducible wedge of the Brillouin zone, integrated by tetrahedron method [28] and a value $R_{MT} = 3.37$ due to the presence of hydrogen.
- [28] P. E. Blochl et al., Phys. Rev. B 49, 16223 (1994).
- [29] FPLO convergence was tested with up to 350 k points in the full Brillouin zone, using the tetrahedron method [28].
- [30] E. Ohmichi et al., J. Phys. Soc. Jpn. 66, 310 (1997).
- [31] The lines are connecting the origin with the results cor-

responding to the tight-binding fit to four LAPW GGA (eight FPLO GGA) bands for -CN and -SCN (-Cl), and the shaded regions containing all other results represent the possible deviation.

[32] R. H. McKenzie, *Comments Condens. Matter Phys.* 18,

309 (1998).

[33] Y. Hayashi, M. Ogata, *J. Phys. Soc. Jpn.* 76, 053705 (2007).

[34] K. Nakamura et al., *arXiv:0903.5409*.